Oxidative Destruction of Dichloromethane over Protonic Zeolites

R. López-Fonseca, S. Cibrián, J. I. Gutiérrez-Ortiz, M. A. Gutiérrez-Ortiz, and J. R. González-Velasco
Dept. de Ingeniería Química, Facultad de Ciencias, Universidad del País Vasco/EHU, E-48080, Bilbao, Spain

Various protonic zeolites (H-Y, H-ZSM-5, and H-MOR) were tested for the total combustion of dichloromethane (DCM) as a model reaction for the catalytic destruction of chlorinated organic pollutants. The order of catalytic activity decreased in the following order: H-MOR > H-ZSM-5 > H-Y. Strong Brønsted acidity played a determining role in controlling the active catalytic behavior as revealed by TPD of ammonia and IR measurements of adsorbed pyridine. DCM oxidative decomposition gave rise to CO and HCl as main products along with small amounts of CO_2 and Cl_2. In addition, methyl chloride was detected as a reaction intermediate between 250 and 500°C. The presence of water in the feed stream led to an inhibition of the zeolite activity and resulted in a noticeable change in the reaction product distribution. Water effectively promoted the selectivity toward environmentally desirable reaction products, that is, HCl and CO_2, and completely suppressed the formation of methyl chloride.

Introduction

Chlorinated volatile organic compounds (VOCs) have been produced commercially and used for many purposes by the chemical industry, including the manufacture of herbicides, plastics, and solvents. Uses outside the chemical industry include solvent degreasing in the automotive and aerospace industries, dry-solvent cleaning solvents in the garment industries, and solvent cleaning in the electronic industries (US EPA, 1991; Sidebottom and Franklin, 1996). However, such compounds constitute a major source of air pollution since they are involved in stratospheric ozone depletion, smog formation, and global warming of the planet. Owing to their high toxicity and ensuing hazardous nature, their proper disposal has become an industrywide concern, and their release into the environment continues to attract considerable concerns, which in turn has led to governmental attempts to control such emissions in many countries (Boubel et al., 1994).

The most widely adopted technique for the treatment of chlorinated VOC-laden effluents is thermal combustion or incineration, which requires temperatures in excess of 1,000°C because of the particular stability of chlorine-containing pollutants (Moretti, 2001). While it is a simple and often cost-effective method of control, the high temperatures required result in a relatively fuel-intensive technique with little control over the ultimate products. The latter is particularly problematic and can lead to incomplete oxidation of the waste stream and the formation of nitrogen oxides and toxic byproducts, if conditions are not carefully controlled. In this sense, Taylor and Dellinger (1998) indicated that pure chlorinated VOCs, when directly combusted with air, tend to yield a large amount of complex chlorinated products of incomplete combustion.

Alternatively, heterogeneous catalytic oxidation offers many potential advantages (Kitrell et al., 1994). The use of a catalyst in the oxidative destruction of chlorinated VOCs significantly lowers the process operating temperature, which is typically in the range of 300–600°C. This reduction in temperature is advantageous, as economically little or no supplementary fuel is required to sustain combustion. In addition, the catalytic process offers a much greater degree of control over the reaction products and can operate with dilute effluent streams (0.1–1% chlorinated VOC), which cannot be treated easily by thermal combustion. Hence, catalytic oxidation can be considered as a more appropriate method of end-of-pipe pollution control. The main requirement is total conversion of chlorine contained in the organic molecule into HCl, and oxidation of the organic part into CO_2 and H_2O.

A prospective catalyst must be active at relatively low temperatures and show high selectivity to carbon oxides and hydrogen chloride. Two broad categories of catalysts usually have been proposed for chlorinated VOCs destruction: noble

---

Correspondence concerning this article should be addressed to J. R. González-Velasco.

metals and metal-oxides-based systems (Spivey, 1987). Noble-metal catalysts, which are often supported, show intrinsic combustion activity; however, they are relatively expensive, susceptible to poisoning by chlorine even at low levels, and in some cases exhibit poor stability. On the other hand, copper, chromium, manganese, and nickel have been used for chlororganics combustion. Generally, it is expected that this type of catalyst can tolerate higher levels of poisons, but the activity shown by these oxides is usually lower than noble-metal-based catalysts. Furthermore, depending on the composition, both noble-metal and metal-oxide catalysts also can be active in the Deacon process and in chlorination reactions, which lead to the formation of molecular chlorine and undesired highly chlorinated compounds. Therefore, the development of catalysts operating at mild conditions for the removal of traces of chlorinated hydrocarbons would be of considerable interest.

Traditionally, H-zeolites have found diverse applications as catalysts in the petrochemical and refining industries owing to their remarkable acidic properties and their shape selectivity; however, much less consideration has given to investigating the suitability of protonic zeolites for abatement of chlorinated VOCs (Prakash et al., 1995; Chintawar and Greene, 1997). Indeed, these few citations in the recent literature revealed the potential characteristics of H-zeolites as effective appropriate catalysts for application in environmental remediation. Protonic zeolites have been shown to exhibit a reasonable destruction activity, being as active as alumina-supported palladium and platinum catalysts in some cases (Aranzabal et al., 2001), together with a high selectivity to hydrogen chloride as a chlorinated oxidation product instead of molecular chlorine. The use of this type of catalyst avoids the eventual incorporation of hazardous transition metal cations such as chromium. In contrast, H-Y zeolites are poor catalysts for the complete conversion to carbon dioxide. Thus, taking into consideration the promising results obtained with chlorinated C_2 ethanes and ethylenes (González-Velasco et al., 2000a; López-Fonseca et al., 2000a,b; López-Fonseca et al., 2001a), a series of protonic zeolites have been investigated for the catalytic decomposition of dichloromethane (DCM), which was selected as a model compound for the general category of chlorinated methanes. Besides, its H/Cl ratio eventually enables the total conversion of Cl into HCl without the presence of other reagents. On the other hand, H-Y, H-ZSM-5 and H-MOR zeolites were chosen as catalysts, since they are three zeolites widely employed on an industrial scale due to their distinct catalytic properties.

Therefore, the main objective of this work is to determine the feasibility of using a range of H-zeolites with different physicochemical properties for the complete combustion of dichloromethane in dry air. The analysis of the influence of water on catalytic activity and product selectivity was included in this study as well.

Experimental

Materials

The zeolites H-Y (CBV400), NH_4-ZSM-5 (CBV5524G), and Na-MOR (CP500C-11) were supplied by the Zeolyst Corporation. The H-Y zeolite was used as received. The H-ZSM-5 zeolite was obtained by calcining the NH_4-ZSM-5 zeolite in air at 550°C for 3 h. The mordenite sample in the NH_4-form was prepared by two successive ion exchanges with a 3-M NH_4NO_3 solution at room temperature for 24 h. The NH_4 form was then transformed to the H form by calcining in air at 550°C for 3 h. The zeolites were pelletized using methylcellulose as a temporary binder, which was removed by calcination in air. Then pellets were crushed and sieved to grains that were 0.3–0.5 mm in diameter.

Zeolite characterization

The determination of the compositions was carried out using a Philips PW 1480 wavelength dispersive X-ray fluorescence (XRF) spectrometer. All the chemical elements were analyzed using a side-window Sc-Mo target X-ray tube and under a vacuum path.

X-ray diffraction (XRD) studies were carried out on a Philips PW 1710 X-ray diffractometer with CuKα radiation ($\lambda = 1.5406$ Å) and Ni filter. The X-ray tube was operated at 30 kV and 20 mA. Samples were scanned from 2θ equal to 2° up to 60°, and the X-ray diffraction-line positions were determined with a step size of 0.02° and a counting time of 2.5 s per step.

The surface areas of the zeolite samples were determined by N_2 adsorption–desorption at −196°C in a Micromeritics ASAP 2010. Samples were previously evacuated overnight at 450°C under high vacuum.

Diffuse reflectance (DRIFT) spectra of pyridine adsorbed on the zeolite samples were obtained with a Nicolet Protegé 460 ESP spectrometer, equipped with a controlled-temperature and environment diffuse reflectance chamber (Spectra-Tech) with KBr windows and a liquid-nitrogen-cooled HgCdTe detector. All spectra were collected in the range of 4,000–1,000 cm^{-1}, averaging 400 scans at an instrumental resolution of 1 cm^{-1}, and analyzed using OMNIC software. Prior to pyridine adsorption the sample was evacuated at 550°C and 10^{-3} $N \cdot m^{-2}$ for 1 h, and then pyridine vapor doses were injected by syringe through a septum until the zeolite sample was saturated. Spectra were recorded at 200°C after 1 h under vacuum in order to reduce the contribution of the gas phase and physisorbed pyridine. Difference spectra were obtained by subtracting the spectrum of the dehydrated zeolite sample from the spectra obtained after pyridine adsorption.

Temperature-programmed desorption (TPD) of ammonia was performed on a Micromeritics AutoChem 2910 instrument. Prior to adsorption experiments, the samples (30–40 mg) were first pretreated in a quartz U-tube in a nitrogen stream at 550°C. Then, they were cooled down at 100°C in a N_2 flow (20 $cm^3 \cdot min^{-1}$) before the ammonia adsorption started. The adsorption step was performed by admitting small pulses of ammonia in Ar at 100°C up to saturation. Subsequently, the samples were exposed to a flow of argon (50 $cm^3 \cdot min^{-1}$) for 2 h at 100°C in order to remove reversibly and physically bound ammonia from the surface. Finally, the desorption was carried out from 100°C to 550°C at a heating rate of 10°C min^{-1} in an Ar stream (50 $cm^3 \cdot min^{-1}$). This temperature was maintained for 15 min until the adsorbate was completely desorbed. A thermal conductivity detector detected the ammonia desorbed. The intensity was first calibrated with ammonia gas in a sample loop.

Catalytic activity measurement

Catalytic oxidation reactions were carried out in a conventional fixed-bed reactor under atmospheric pressure (González-Velasco et al., 1998). The reactor consisted of a 1.2-cm-ID stainless-steel tube approximately 25 cm long. The catalyst bed (0.85 g, 2 cm^3) was supported on a plug of glass wool located 9 cm from the bottom of the reactor. Two-mm-OD crushed quartz glass was placed above the catalyst bed to serve as a preheat zone for the incoming feed stream. The temperature was measured with a type-K thermocouple, whose control scheme allowed for maintaining a stable bed temperature to within ± 1°C of the desired value. The reactor was housed in a 26-cm-diameter by 42-cm-long electrically heated furnace, which provided uniform heating of the catalyst bed.

The flow rate through the reactor was set at 500 $cm^3 \cdot min^{-1}$, and the gas hourly space velocity (GHSV) was maintained at 15,000 h^{-1} (Keller and Dyer, 1998). The residence time based on the packing volume of the catalyst was 0.24 s. Dry, oil-free air delivered from a PSA air drier was metered to the system using a mass flow controller of the appropriate range. The liquid chlorinated hydrocarbon (1,000 ppm) and water (15,000 ppm) were injected into the dry air using syringe pumps. The point of liquid injection was electrically heated in order to ensure complete evaporation of both reactants. Before entering the reactor, the feed stream was homogeneously blended in a 2 dm^3 static mixer, which served to dampen out possible oscillations of the syringe pumps as well. Subsequently, the temperature was raised from 200°C to 550°C in steps of 50°C, and conversion measurements and product profiles were taken at steady state, typically after 20 min on stream. Teflon tubing was employed due to its insensitivity to corrosion by hydrogen chloride.

Following the reactor, a portion of the effluent stream was delivered and analyzed on-line using a Hewlett-Packard 5890 Series II gas chromatograph (GC) equipped with an electron capture detector (ECD) and a thermal conductivity detector (TCD). CO and CO_2 were separated using both a 0.6-m-long $\times$0.32-cm-OD 13X molecular sieve column and a 2.4-m-long $\times$ 0.32-cm-OD Hayesep N column interconnected to a gas sampling loop by a single 10-port valve and were analyzed using a TCD. The concentration of the chlorinated feeds and any other chlorinated hydrocarbons formed in the reaction were determined by the ECD after being separated in an HP-VOC column. The GC was previously calibrated for reaction product response. Reactor effluent was also quantitatively analyzed for phosgene using Dräger tubes. Analyses were performed for selected runs by attaching the Dräger tube directly to the reactor outlet using a short piece of Teflon tubing. In this way, the entire feed stream was passed through the Dräger tube. The tube was removed after a known volume of gas has passed through the tube.

Table 1. Physicochemical Properties of the Zeolite Catalysts

Zeolite	Total Acidity ($mmol\ NH_3\ g^{-1}$)	Weak Sites ($mmol\ NH_3\ g^{-1}$)	Strong Sites* ($mmol\ NH_3\ g^{-1}$)
H-Y	0.65	0.56	0.09
H-ZSM-5	0.49	0.22	0.27
H-MOR	1.18	0.79	0.39

*Sites retaining ammonia at temperatures higher than 250°C

Analysis of both Cl_2 and HCl was performed by bubbling the effluent stream through a 0.0125-N NaOH solution. The Cl_2 concentration was determined by titration with ferrous ammonium sulfate (FAS) using *N*,*N*-diethyl-*p*-phenylenediamine (DPD) as an indicator. The concentration of chloride ions in the bubbled solution was determined by using an ion selective electrode.

Results and Discussion

Zeolite characterization

Table 1 lists the main physicochemical properties, that is, surface area, Si/Al ratio, pore volume, and micropore volume, of the H-zeolites examined in this work. According to the IUPAC recommendations, the BET surface area (S_{BET}) would be better called "monolayer equivalent surface area" in the case of microporous materials. Whatever the difference between the BET theory (a theory established for nonmicroporous solids) and the Dubinin theory (a theory developed to characterize solids containing micropores), it is reported that results (micropore volume and surface area) obtained from both theories, although not identical, are linearly correlated. This result justifies to some extent the wide use of S_{BET} and V_{micro} in order to make comparison among different zeolite materials (Raatz and Ajot, 1987). The calculated values of the textural properties were in agreement with those found in the literature for this type of materials (Breck, 1974; Remy and Poncelet, 1995).

Temperature-programmed desorption of a base molecule is a convenient method for determination of the acidic properties of solid catalysts (Marcelin, 1993). It is generally recognized that ammonia is an excellent molecule of TPD because it can be stabilized on acid sites and can penetrate into pores due to its strong basicity and small size. Not only the overall acidity but also the distribution of acid strength can be surmised from the NH_3-TPD profile. On the other hand, the adsorption of base probes, mainly pyridine, followed by infrared spectroscopy shows the nature of the acid sites discriminating Brønsted and Lewis sites (Busca, 1998).

Figure 1 shows the diffuse-reflectance infrared spectra of pyridine adsorbed on the zeolites at 200°C in the region 1,700–1,400 cm^{-1} at 10^{-3} $N \cdot m^{-2}$. The absorption band around 1,545 cm^{-1} is assumed to be characteristic for pyridinium ions, while absorption bands between 1,445 and 1,460 cm^{-1} are attributed to coordinatively adsorbed pyridine. The band at 1,492 cm^{-1} can be assigned to pyridine associated with Brønsted and Lewis sites (Lercher et al., 1996). In the literature, the bands at 1,545 and 1,450 cm^{-1} are used for the determination of Brønsted and Lewis sites, respectively (Barzetti et al., 1996). The samples exhibited both Brønsted and Lewis acidity. H-Y presented a large number of both types of acid sites, while H-ZSM-5 and H-MOR predominantly contained Brønsted sites, as the absorption band at 1,450 cm^{-1} attributed to pyridine bonded to Lewis sites was very low.

The results from the acidity determination experiments are plotted in Figure 2. The NH_3 desorbed above 100°C was considered as chemisorbed NH_3 and subsequently used for acidity determination. The amount of adsorbed NH_3 was 0.97, 0.65, and 0.49 $mmol \cdot g^{-1}$ for H-MOR, H-Y, and H-ZSM-5, respectively. As expected, H-ZSM-5 showed the lowest total

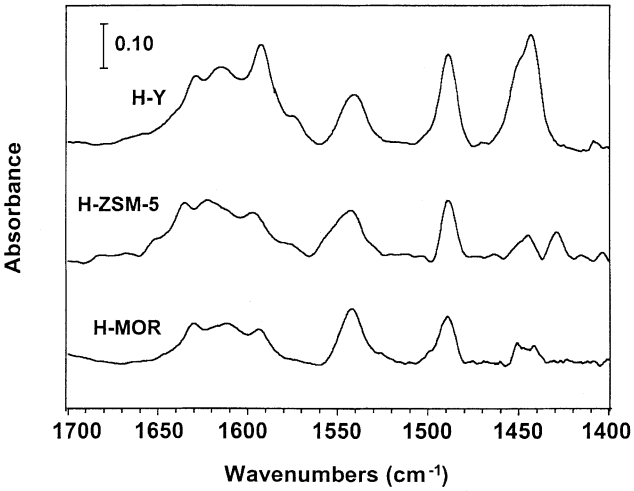

Figure 1. IR spectra of adsorbed pyridine on H-zeolites.

acidity due to its low aluminum content (Chen et al., 1992). The position of the temperature maximum in the plot of the ammonia desorption vs. temperature was an indication of the magnitude of the NH_3 desorption activation energy, and consequently the relative acid strength of the sites. As can be seen in Figure 2, all the curves displayed a major desorption peak around 150°C, which is indicative of the weak (Brønsted and/or Lewis) sites present in the zeolite catalysts. Apart from the maximum temperature of the NH_3 desorption curve, the area under the desorption peak was also indicative of the relative number of acid sites present. Comparing the desorption curves of the different catalysts (Table 2), it was found that the apparent number of weak sites was noticeably larger (around 85% of the total acid sites) in H-Y compared with those of H-ZSM-5 (about 45%) and H-MOR (around 55%).

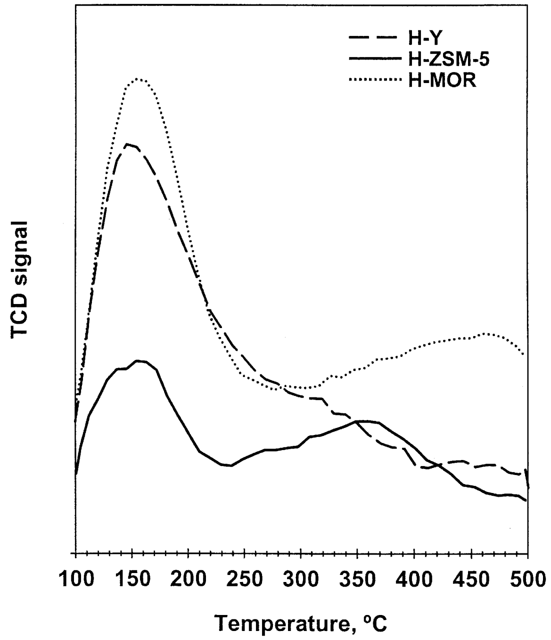

Figure 2. Temperature-programmed desorption of ammonia from H-zeolites.

Table 2. Total Acidity and Acid Strength Distribution of the Zeolite Catalysts

	Si/Al	Surface Area ($m^2 \cdot g^{-1}$)	V_{pore} ($cm^3 \cdot g^{-1}$)	$V_{\text{micropore}}$ ($cm^3 \cdot g^{-1}$)
H-Y	2.4	900	0.382	0.312
H-ZSM-5	27.3	460	0.230	0.147
H-MOR	5.2	570	0.223	0.203

A second much smaller desorption peak was obtained for H-ZSM-5 (350°C) and H-MOR (450°C) in the range of 350–450°C, indicating the presence of strong Brønsted acid sites. On the contrary, H-Y showed a much smaller inflection in this region. According to the TPD profiles H-ZSM-5 zeolite contained acidic hydroxyl groups similar to those existing in H-MOR. The acid strength of H-MOR was slightly higher than that of H-ZSM-5, the two zeolites differing mainly by the number of acid sites, which was larger in H-MOR (Hidalgo et al., 1984).

Transport effects

Before testing the activity and selectivity of the zeolite catalysts, the transport effects were evaluated to ensure that experimental results were not significantly influenced by interphase transportation (Satterfield, 1970). External mass- and heat-transfer resistances were evaluated using a criteria outlined by Mears (1971). The j factor was calculated using equations presented by Froment and Bischoff (1990), and, as an approximation, j_d, was assumed to be equal, j_h. The remaining physical properties were obtained from Reid et al. (1987). The criteria of Mears were satisfied for elimination of both external mass- and heat-transfer resistances. Likewise, calculation of the theoretical external transfer rate of reactants to the catalytic particles (at a typical temperature of 400°C) based on estimated mass-transfer coefficients gave a value three orders of magnitude larger than the measured reaction rates, indicating process conditions are far from external diffusion limitations. The effects of external mass-transfer resistances were experimentally evaluated by repeating a set of process conditions while employing a different linear velocity. Results of these experiments indicated that conversion was not affected for linear velocity higher than 7 $cm \cdot s^{-1}$, to within the experimental error. Estimates of interphase temperature gradients showed fluid–solid differences of less than 2°C, thereby limiting heat-transfer limitation concerns.

Although the temperature profile within the catalyst bed could not be monitored, deviation from isothermal operation could be assessed by comparing the catalyst-bed temperature to that of the ceramic block surrounding the catalyst prior to and following reactant exposure. In all cases, the increase in the catalyst-bed temperature was less than 1–2°C, indicating that axial temperature gradients were not influencing the experimental results.

The possibility of internal pore diffusion was examined by measuring conversions at fixed conditions for catalyst particles of different size, and the results showed that pore diffusion resistance was absent for particles less than 1 mm in diameter. Intraparticle mass-transfer resistances were theoretically evaluated by computing effectiveness factors, which

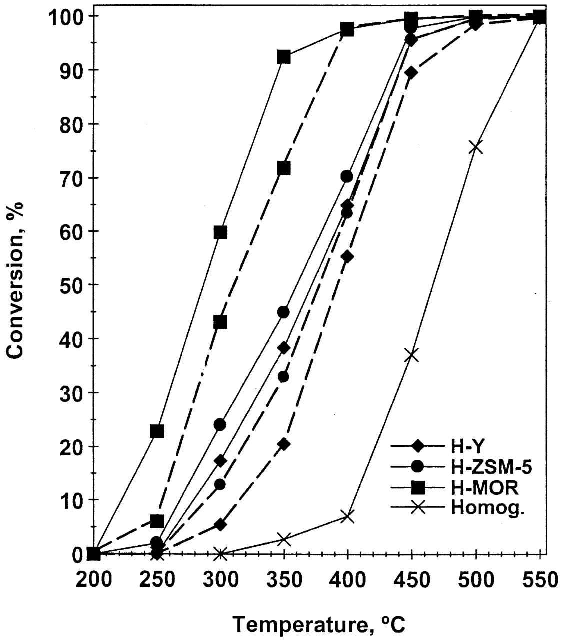

Figure 3. Dichloromethane destruction light-offs under dry (solid lines) and humid conditions (dashed lines).

were calculated to be greater than 0.98, indicating that intraparticle mass-transfer resistances were not significant. Likewise, internal thermal gradients were found not to be contributing to the observed conversion over the range of conditions evaluated in this study.

Catalytic activity results

The oxidation destruction activity of a catalyst is best illustrated by analyzing the conversion as a function of temperature, which is known as a light-off curve. Figure 3 shows the light-off curves for dry DCM decomposition for the various zeolites examined in this work (solid lines). Likewise, the curve corresponding to the destruction of a chlorinated compound without any catalyst is included for the sake of comparison. The extent to which homogeneous oxidation of DCM occurred was determined by an experiment placing crushed quartz glass into the reactor tube. As can be observed, all three zeolites converted the chlorinated hydrocarbon at temperatures markedly lower than the homogeneous combustion. This result revealed the ability of protonic zeolites to decompose chlorine-containing compounds.

According to the destruction activity, the zeolites could be listed as H-MOR > H-ZSM-5 > H-Y. Tajima et al. (1996) examined several solid acid catalysts for the decomposition of chlorofluorocarbons (CFCs) and found H-zeolites as active catalysts. In fact, H-type zeolites exhibited the highest activity among the catalysts tested, and the catalytic behavior followed the same trend showed in this work. These results were also in good agreement with those reported by Nagata et al. (1994) when testing several H-type zeolites for the destruction of CFCs. On the other hand, Greene et al. (1996) also found H-ZSM-5 more reactive than H-Y zeolite in the oxidation of carbon tetrachloride.

The T_{50} (temperature at which 50% conversion is achieved) values for DCM combustion were 280, 360 and 375°C over H-MOR, H-ZSM-5, and H-Y, respectively. In contrast, homogeneous reaction was only noticed at temperatures higher than 400°C, and a minimum temperature of 475°C was required for achieving 50% conversion. Ballykaya et al. (1996) also reported homogeneous decomposition of DCM above 400°C. Hence, the use of protonic zeolites as catalysts represented a drop in T_{50} values ranging from 100°C to 200°C, depending on the type of zeolite catalyst employed. The complete oxidation was attained above 400°C over H-MOR zeolite, while H-ZSM-5 and H-Y required 450°C.

It must be pointed out that the temperature needed for the decomposition of DCM was significantly higher than those required for the destruction of chlorinated ethanes (González-Velasco et al., 2000a), which proved that DCM was a noticeably refractory chlorinated VOC in comparison with compounds with larger carbon–carbon linkages. Several authors have mentioned the preferable destruction of chlorinated ethanes with respect to chloromethanes (Windawi and Wyatt, 1993; Jang et al., 1998). On the other hand, it has been highlighted that the relative ease of destruction of chloromethanes increased as the number of chlorine atoms increased (Petrosius et al., 1993; Lester, 1999).

According to the results obtained from the acidity characterization and the catalytic tests, strong Brønsted acidity appears to play a key role in determining the catalytic behavior of H-type zeolites (Prakash et al., 1995; González-Velasco et al., 2000a). Zeolite catalytic activity correlated with the number of strong sites present in the samples (Table 2). It is widely accepted that the combustion of chlorinated hydrocarbons is initiated by proton transfer from the Brønsted sites to the adsorbate molecule as a first step in the reaction scheme (Chatterjee et al., 1992; Konya et al., 1996). Therefore, a site having stronger acidity should show higher/stronger chlorinated VOC adsorption and consequently show a higher destruction activity. Oxygen was assumed to react from the gas phase with adsorbed dichloromethane since no appropriate sites for oxygen adsorption are present in metal-free protonic zeolites.

It is worth noting that the surface area of the zeolites did not appear to control the activities of the catalysts, as significant differences in the surface-area values, as listed in Table 1, were observed with no corresponding trend in activity.

The main oxidation products in the decomposition of DCM were carbon monoxide and hydrogen chloride, while carbon dioxide and molecular chlorine were minor products (Figure 4). Interestingly, no phosgene ($COCl_2$) was detected in the product stream of any zeolite catalyst. The absence of this extremely toxic byproduct was confirmed by the use of Dräger tubes. In addition, the reaction of DCM was accompanied by the substantial formation of methyl chloride (Figure 5). Hence, as soon as DCM started to react at 200°C over H-MOR and at 250°C over H-ZSM-5 and H-Y, the generation of methyl chloride was detected. The concentration of this byproduct increased, with temperature being maximum at 350°C over H-MOR and at 400°C over H-ZSM-5 and H-Y. The peak concentration of this byproduct was around 380, 195 and 160 ppm over H-MOR, H-ZSM-5, and H-Y zeolites, respectively. At higher temperatures the concentration decreased, and thus this byproduct was completely decomposed

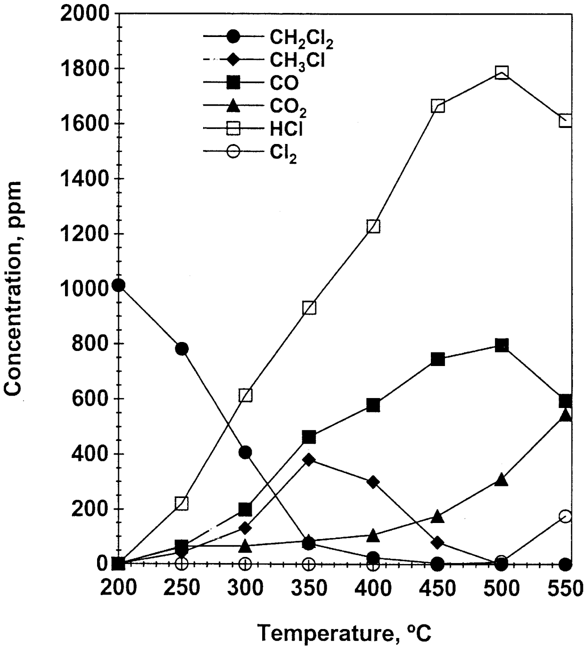

Figure 4. Product distributions from dichloromethane decomposition over H-MOR zeolite under dry conditions.

at 500°C. No additional chlorinated organic product was detected in the product stream of any catalyst. Methyl chloride was also noticed during the combustion of DCM over γ-alumina (van den Brink et al., 1998; Haber et al., 1999). Similarly, Storaro et al. (1997) found substantial amounts of this product over pillared clay materials.

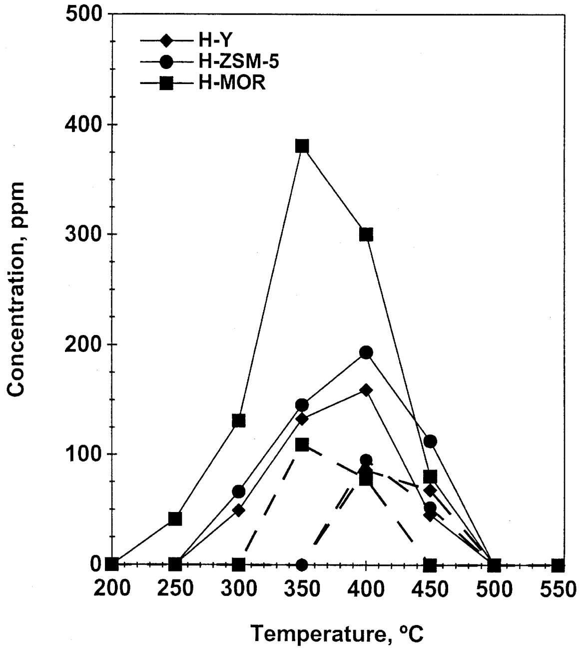

Figure 5. Methyl chloride concentrations in the absence (solid lines) and presence of water (dashed lines).

The formation of chlorinated organic byproducts has been amply studied, since their environmental impact is sometimes higher than that of the starting material. In this sense, Schneider et al. (1999) and Sinquin et al. (2000), when using perovskite-based catalysts for the conversion of DCM, noticed large amounts of highly chlorinated byproducts such as $CHCl_3$ and CCl_4. Also, these compounds were produced during the combustion of DCM with chromia-based catalysts (Padilla et al., 1999).

DCM contains sufficient hydrogen associated with the parent molecule to yield hydrogen chloride exclusively. Unexpectedly, a significant quantity of molecular chlorine was observed above 450°C. The Cl_2 is believed to arise from the oxidation of hydrogen chloride at high temperatures, the Deacon reaction ($2HCl + 1/2O_2 \rightleftharpoons Cl_2 + H_2O$). The formation of HCl is preferable to Cl_2 because hydrogen chloride is less toxic and is more easily removed from the effluent stream, thereby reducing problems in downstream processing equipment. Conversely, metal-loaded catalysts are claimed to be highly active for the Deacon reaction, resulting in the generation of undesired chlorine (Janas et al., 2000). The maximum chlorine concentration at 550°C was 300, 210 and 145 ppm over H-ZSM-5, H-MOR, and H-Y, respectively. However, almost 400 ppm was noticed when oxidizing with the catalyst substituted by inert quartz glass. This suggested that the notable presence of OH groups in the zeolite structures was likely to inhibit to a certain extent the conversion of HCl to Cl_2 (López-Fonseca et al., 2001b).

As mentioned earlier, it is believed that initially DCM adsorbs on the Brønsted site giving rise to the carbonium ion. Hence, in order to obtain insights on the surface phenomena in the reaction process, DCM adsorption on H-ZSM-5 zeolite sample was analyzed by means of *in situ* DRIFT spectroscopy. The infrared spectra of the zeolite hydroxyls are shown in Figure 6 during DCM adsorption at different temperatures. In the spectrum of the H-ZSM-5 sample pretreated at 500°C in vacuum, two absorption bands were observed at 3,740 cm^{-1} attributed to nonacidic terminal silanols and at 3,609 cm^{-1} assigned to Brønsted acid sites, that is, a hydroxyl group bridging between silicon and aluminium within the zeolite pores. An additional small absorption band, which was associated with AlOH groups involving partially extraframework alumina species (Buzzoni et al., 1996), was detected at 3,670 cm^{-1}. By admitting DCM onto the sample the band at 3,609 cm^{-1} completely disappeared, while the band at 3,740 cm^{-1} remained intact. This interaction was studied by following the restoration of the band at 3,609 cm^{-1} upon desorbing DCM in vacuum at increasing temperatures. The results showed that the IR band was recovered only after heating at about 300°C. This behavior clearly indicated that Brønsted acid sites acted as effective chemisorption sites for DCM.

Ramachandran et al. (1996) investigated the DCM destruction mechanism on Co-Y catalyst by infrared spectroscopy and proposed abstraction of zeolite hydroxyls leading to the formation of HCl. The carbonium ion next formed the carbenium ion by the abstraction of a molecule of hydrogen chloride (Ramachandran et al., 1996). Similarly, Konya et al. (1996) studied the interaction of CH_3Cl with zeolites and observed a process with a hydroxyl group to produce gaseous HCl. The unstable carbenium ion possibly interacted with

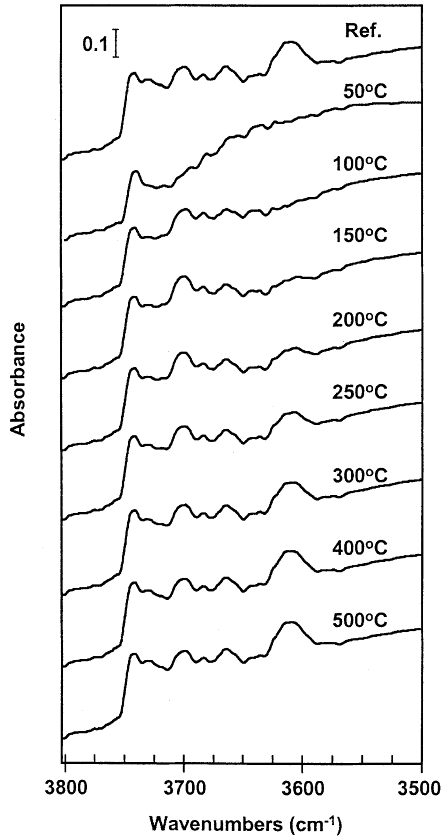

Figure 6. Diffuse-reflectance IR spectra of DCM adsorbed on H-ZSM-5 zeolite at different temperatures.

gas-phase oxygen, producing CO, CO_2, and HCl, and resulting in the restoration of the Brønsted site. Although metal-loaded zeolites can offer cationic sites for dissociative adsorption of oxygen, no sites for oxygen adsorption are available in pure protonic zeolites. Furthermore, catalytic runs performed in nitrogen atmosphere revealed a very low DCM conversion. Methyl chloride measured during reaction was assumed to be formed by the replacement of a chlorine atom by a hydrogen atom (hydrodechlorination) in the feed molecule. This byproduct was decomposed at high temperatures.

As said previously, substantial amounts of carbon monoxide were generated in the decomposition of DCM over the zeolite catalysts (Figure 7). The common feature of the formation of CO as an oxidation product was expected, since H-zeolites lack active sites for CO oxidation. It was noted that increasing reaction temperature always increased the catalytic selectivity toward carbon dioxide formation as CO homogeneous oxidation was promoted. Jiang et al. (1996) found that CO was favored in the oxidation of methylene chloride over acidic sulfated oxide catalysts. Analogously, Feaver and Rossin (1999) observed that CO predominated over CO_2 during CHF_3 conversion over ZrO_4-SO_4 catalysts.

Effect of water addition on catalytic activity and product selectivity

Catalytic runs were also conducted in the presence of water vapor, since water is present in significant quantities in the flue gases of different combustion processes and has been found to affect both catalytic performance and distribution of the decomposition products. The concentration of water vapor in a gas effluent stream can easily exceed the concentration of chlorinated VOCs. In the case of streams from air stripping in contaminated groundwater, the water concentration can be higher than 10,000 ppm. In this work, a reaction feed containing 1,000 ppm DCM plus 15,000 ppm H_2O was employed. Figure 3 shows the light-off curves of DCM combustion under humid conditions (dashed lines). The presence of water in the feed stream was found not to alter the order of catalytic activity of the zeolites observed under dry conditions. It could be seen that water indeed acted as an inhibitor of chlorinated VOC decomposition, and the inhibiting effect of water appeared to be comparable on all the zeolites. Hence, T_{50} values increased from 280°C to 310°C over H-

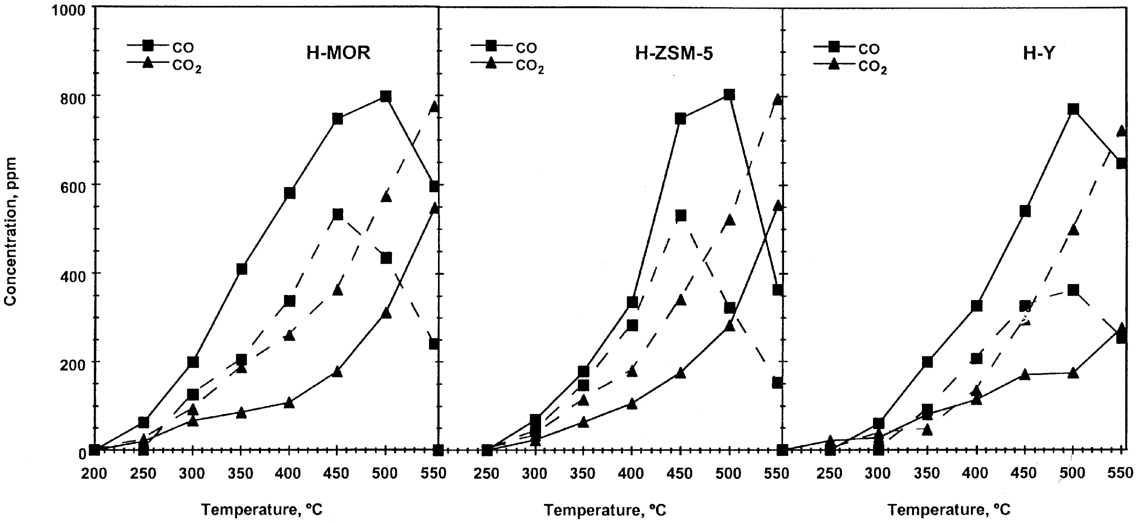

Figure 7. Carbon monoxide and carbon dioxide concentrations in the absence (solid lines) and presence (dashed lines) of water.

MOR, from 360°C to 370°C over H-ZSM-5, and from 375°C to 390°C over H-Y. The drop in catalytic activity in the presence of excess of water has been reported in the literature (Freidel et al., 1993; Rossin and Farris, 1993). This inhibition by water probably reflected the competition of the reactant molecules with water molecules for adsorption on the active sites. Water molecules may also create a diffusion blockage for DCM molecules, resulting in low catalytic activity. The influence of water on the catalytic performance was more pronounced for H-MOR and H-Y zeolites. The decrease in conversion observed for these two zeolites is attributed to the strong hydrophilic character of aluminum-rich zeolites. This is in contrast with the behavior of zeolites with a high Si/Al ratio, such as H-ZSM-5, which are markedly hydrophobic, and therefore offer reduced sensibility to water inhibition (Chen, 1976).

The presence of water also noticeably changed the reaction-product distribution. On the one hand, the generation of methyl chloride was found to be significantly suppressed (Figure 5). Besides, the temperature at which this compound was generated was retarded about 100°C with respect to the runs carried out in the absence of water. The peak concentration diminished from 380 ppm under dry conditions to 110 ppm under humid conditions over H-MOR, from 195 to 50 ppm over H-ZSM-5, and from 160 to 85 ppm over H-Y. The inhibiting effect of water on the formation of reaction intermediates was consistent with previous reports on DCM oxidation (van den Brink et al., 1998; Sinquin et al., 2000). On the other hand, upon adding 15,000 ppm of water to the feed stream, virtually no molecular chlorine was detected, with HCl being the predominant chlorine-containing product in the effluent stream. It is thought that water could inhibit the Deacon reaction, and provides the hydrogen needed for the formation of the desired product HCl (Chen et al., 1996; González-Velasco et. al., 2000b; Pinard et al., 2001). Additionally, Figure 7 shows that the addition of water to the reaction mixture caused a significant shift in the product selectivity toward CO_2 (Jiang et al., 1996).

Carbon balances were typically greater than 90% for all runs reported in this study. Nevertheless, it was noticed that the chlorine balance was in the range of 75–90% under dry conditions, whereas it was in the range of 65–80% for the catalytic experiments performed in the presence of water. It is known that Al-O bonds in the zeolite framework can be easily attacked by the HCl formed during reactions leading to the formation of $AlCl_3$ that could be retained in the zeolite pellet (Konya et al., 1996). This halogen deactivation causes the partial collapse of the framework and the blockage of the porous structure, and it is noticeably enhanced by the presence of water. XRD measurements of the zeolite catalysts after reaction revealed that the H-ZSM-5 sample showed the highest resistance to halogen deactivation, since no noticeable decrease in crystallinity was observed. On the contrary, the crystallinity of the spent H-Y and H-MOR zeolites decreased to 80–85% due to their higher aluminum content in comparison with that of H-ZSM-5 zeolite.

Conclusions

Three protonic zeolites (H-Y, H-ZSM-5, and H-MOR) were successfully examined for the oxidative destruction of DCM in both dry and humid gas streams. The catalytic performance followed the trend: H-MOR > H-ZSM-5 > H-Y. According to the zeolite characterization, strong Brønsted acidity was found to play a key role in determining the active behavior of the zeolites, since Brønsted acid sites are believed to act as effective sites for DCM adsorption. DCM combustion led to the formation of carbon monoxide and hydrogen chloride as major reaction products. The combustion process was also accompanied by the generation of small amounts of methyl chloride, carbon dioxide, and molecular chlorine.

Zeolite activity was observed to be inhibited by the presence of an excess of water vapor. As far as the nature of the reaction products was concerned, water addition enhanced the formation of carbon dioxide and inhibited the Deacon reaction, resulting in the almost exclusive formation of hydrogen chloride. Likewise, the yield of methyl chloride was significantly reduced.

Acknowledgments

The authors thank Universidad del País Vasco/EHU (9/UPV 0069.310-13517/2001) and Ministerio de Ciencia y Tecnología (PPQ2001-0543) for the financial support.

Literature Cited

Aranzabal, A., R. López-Fonseca, J. R. González-Velasco, J. I. Gutiérrez-Ortiz, M. A. Gutiérrez-Ortiz, and J. A. González-Marcos, "Development of an Active and Environmentally Selective Bifunctional Metal-Zeolite Catalyst for Chlorinated VOC Abatement," *Abstr. Pap.—221st Amer. Chem. Soc.*, CATL-027 (2001).

Ballikaya, M., S. Atalay, H. E. Alpay, and F. S. Atalay, "Catalytic Combustion of Methylenechloride," *Combust. Sci. Technol.*, **120**, 169 (1996).

Barzetti, T., E. Selli, D. Moscotti, and L. Forni, "Pyridine and Ammonia as Probes for FTIR Analysis of Solid Acid Catalysts," *J. Chem. Soc., Faraday Trans.*, **92**, 1401 (1996).

Boubel, R. W., D. L. Fox, D. B. Furner, and A. C. Stern, *Fundamentals of Air Pollution*, Academic Press, San Diego (1994).

Breck, D. W., *Zeolite Molecular Sieves: Structure, Chemistry and Use*, Wiley, New York (1974).

Busca, G., "Spectroscopic Characterization of the Acid Properties of Metal Oxide Catalysts," *Catal. Today*, **41**, 191 (1998).

Buzzoni, R., S. Bordiga, G. Ricchiardi, C. Lamberti, A. Zecchina, and G. Bellusi, "Interaction of Pyridine with Acidic (H-ZSM5, H-β, H-MORD Zeolites) and Superacidic (H-Nafion Membrane) Systems: An IR Investigation," *Langmuir*, **12**, 930 (1996).

Chatterjee, S., H. L. Greene, and Y. K. Park, "Comparison of Modified Transition Metal-Exchanged Zeolite Catalysts for Oxidation of Chlorinated Hydrocarbons," *J. Catal.*, **138**, 179 (1992).

Chen, B., C. Bai, R. Cook, J. Wright, and C. Wang, "Gold/Cobalt Oxide Catalysts for Oxidative Destruction of Dichloromethane," *Catal. Today*, **30**, 15 (1996).

Chen, D. T., S. B. Sharma, I. Filimonov, and J. A. Dumesic, "Microcalorimetric Studies of Zeolite Acidity," *Catal. Lett.*, **12**, 201 (1992).

Chen, N. Y., "Hydrophobic Properties of Zeolites," *J. Phys. Chem.*, **80**, 60 (1976).

Chintawar, P. S., and H. L. Greene, "Adsorption and Catalytic Destruction of Trichloroethylene in Hydrophobic Zeolites," *Appl. Catal. B*, **14**, 37 (1997).

Feaver, W. B., and J. A. Rossin, "The Catalytic Decomposition of CHF_3 over ZrO_2-SO_4," *Catal. Today*, **54**, 13 (1999).

Freidel, J. M., A. C. Frost, K. J. Herbert, F. J. Meyer, and J. C. Summers, "New Catalyst Technologies for the Destruction of Halogenated Hydrocarbons and Volatile Organics," *Catal. Today*, **17**, 367 (1993).

Froment, G. F., and K. B. Bischoff, *Chemical Reactor Analysis and Design*, Wiley, New York (1990).

González-Velasco, J. R., R. López-Fonseca, A. Aranzabal, J. I. Gutiérrez-Ortiz, and P. Steltenpohl, "Evaluation of H-type Zeolites in the Destructive Oxidation of Chlorinated Volatile Organic Compounds," *Appl. Catal. B*, **24**, 233 (2000a).

González-Velasco, J. R., A. Aranzabal, R. López-Fonseca, R. Ferret, and J. A. González-Marcos, "Enhancement of the Catalytic Oxidation of Hydrogen-Lean Chlorinated VOCs in the Presence of Hydrogen-Supplying Compounds," *Appl. Catal. B*, **24**, 33 (2000b).

González-Velasco, J. R., A. Aranzabal, J. I. Gutiérrez-Ortiz, R. López-Fonseca, and M. A. Gutiérrez-Ortiz, "Activity and Product Distribution of Alumina Supported Platinum and Palladium Catalysts in the Gas-Phase Oxidative Decomposition of Chlorinated Hydrocarbons," *Appl. Catal. B*, **19**, 189 (1998).

Greene, H., D. Prakash, K. Athota, G. Atwood, and C. Vogel, "Energy Efficient Dual-Function Sorbent/Catalyst Media for Chlorinated VOC Destruction," *Catal. Today*, **27**, 289 (1996).

Haber, J., T. Machej, M. Derewinski, R. Janik, J. Krysciak, H. Sadowska, and J. Janas, "Catalytic Oxidation of CH_2Cl_2 on Sodium Doped Al_2O_3," *Catal. Today*, **54**, 47 (1999).

Hidalgo, C. V., H. Itoh, T. Hattori, M. Niwa, and Y. Murakami, "Measurement of the Acidity of Various Zeolites by Temperature-Programmed Desorption of Ammonia," *J. Catal.*, **85**, 362 (1984).

Janas, J., R. Janik, T. Machej, E. M. Serwicka, E. Bielánska, E. Bastardo-González, and W. Jones, "Cr-Doped Zr, Si-Mesoporous Molecular Sieves as Catalysts of CH_2Cl_2 Oxidation," *Catal. Today*, **59**, 241 (2000).

Jang, B. H., S. S. Lee, T. H. Yeon, and J. E. Yie, "Effects of Base Metal Promoters in VOC Catalysts for Chlorocarbons and n-Hexane Oxidation," *Korean J. Chem. Eng.*, **15**, 516 (1998).

Jiang, X. Z., L. Q. Zhang, X. H. Wu, and L. Zheng, "Catalytic Decomposition of Methylene Chloride by Sulphated Oxide Catalysts," *Appl. Catal. B*, **9**, 229 (1996).

Keller, R. A., and J. A. Dyer, "Abating Halogenated VOCs," *Chem. Eng.*, **105**, 100 (1998).

Kitrell, J. R., C. W. Quinian, and J. W. Eldridge, "Direct Catalytic Oxidation of Halogenated Hydrocarbons," *J. Air Waste Manage. Assoc.*, **41**, 1129 (1991).

Konya, Z., I. Hannus, and I. Kiricsi, "Infrared Spectroscopic Study of Adsorption and Reactions of Methyl Chloride on Acidic, Neutral and Basic Zeolites," *Appl. Catal. B*, **8**, 391 (1996).

Lercher, J. A., C. Grüdling, and G. Eder-Mirth, "Infrared Studies of the Surface Acidity of Oxides and Zeolites Using Adsorbed Probe Molecules," *Catal. Today*, **27**, 353 (1996).

Lester, G., "Catalytic Destruction of Hazardous Halogenated Organic Chemicals," *Catal. Today*, **53**, 407 (1999).

López-Fonseca, R., J. R. González-Velasco, A. Aranzabal, J. I. Gutiérrez-Ortiz, and P. Steltenpohl, "H-Type Zeolite Catalysts for the Oxidative Decomposition of C_2 Chlorinated Hydrocarbons," *Proc. of Industrial Applications of Zeolites*, Technologisch Instituut, Brugge, Belgium, p. 223 (2000a).

López-Fonseca, R., A. Aranzabal, P. Steltenpohl, J. I. Gutiérrez-Ortiz, and J. R. González-Velasco, "Performance of Zeolites and Product Selectivity in the Gas-Phase Oxidation of 1,2-Dichloroethane," *Catal Today*, **62**, 367 (2000b).

López-Fonseca, R., A. Aranzabal, J. I. Gutiérrez-Ortiz, J. I. Álvarez-Uriarte, and J. R. González-Velasco, "Comparative Study of the Oxidative Decomposition of Trichloroethylene over H-Type Zeolites Under Dry and Humid Conditions," *Appl. Catal. B*, **30**, 303 (2001a).

López-Fonseca, R., J. I. Gutierrez-Ortiz, A. Aranzabal, and J. R. Gonzalez-Velasco, "Analysis of the Deep Catalytic Oxidation of Binary CVOCs Mixtures Over H-ZSM-5 Zeolite," *Stud. Surf. Sci. Catal.*, **135**, 4995 (2001b).

Marcelin, G., "Techniques for Measuring Zeolite Acidity," *Catalysis*, **10**, 83 (1993).

Mears, D. E., "Tests for Transport Limitations in Experimental Catalytic Reactors," *Ind. Eng. Chem. Process Des. Dev.*, **10**, 71 (1971).

Moretti, E. C., *Practical Solutions for Reducing Volatile Organic Compounds and Hazardous Air Pollutants*, CWRT AIChE, New York (2001).

Nagata, H., T. Takakura, S. Tashiro, M. Kishida, K. Mizuno, I. Tamori, and K. Wakabayashi, "Catalytic Oxidative Decomposition of Chlorofluorocarbons (CFCs) in the Presence of Hydrocarbons," *Appl. Catal. B*, **5**, 23 (1994).

Padilla, A. M., J. Corella, and J. M. Toledo, "Total Oxidation of Some Chlorinated Hydrocarbons With Commercial Chromia Based Catalysts," *Appl. Catal. B*, **22**, 107 (1999).

Petrosius, S. C., R. S. Drago, V. Young, and G. C. Grunewald, "Low-Temperature Decomposition of Some Halogenated Hydrocarbons Using Metal Oxide/Porous Carbon Catalysts," *J. Amer. Chem. Soc.*, **115**, 6131 (1993).

Pinard, L., J. Tsou, P. Magnoux, and M. Guisnet, "Catalytic Destruction of Chlorinated VOCs. Influence of Characteristics of Pt/FAU Catalysts on the Destruction of Dichloromethane," *Stud. Surf. Sci. Catal.*, **135**, 4995 (2001).

Prakash, D. S., K. V. Athota, H. L. Greene, and C. A. Vogel, "Sorption and Catalytic Destruction of Chlorinated VOCs Using Fresh and Dealuminated Y and ZSM-5 Zeolites," *AIChE Symp. Ser.*, **91**, 1 (1995).

Raatz, F., and H. Ajot, "Characterization of Microporous Catalysts by Nitrogen Adsorption: Empirical Correlations Between Parameters Assessed by Different Methods," *Stud. Surf. Sci. Catal.*, **39**, 119 (1987).

Ramachandran, B., H. L. Greene, and S. Chatterjee, "Decomposition Characteristics and Reaction Mechanisms of Methylene Chloride and Carbon Tetrachloride Using Metal-Loaded Zeolite Catalysts," *Appl. Catal. B*, **9**, 157 (1996).

Reid, R. C., J. M. Prausnitz, and B. E. Poling, *The Properties of Gases & Liquids*, McGraw-Hill, New York (1995).

Remy, M. J., and G. Poncelet, "A New Approach to the Determination of the External Surface and Micropore Volume of Zeolites From the Nitrogen Adsorption Isotherm at 77 K," *J. Phys. Chem.*, **99**, 773 (1995).

Rossin, J. A., and M. M. Farris, "Catalytic Oxidation of Chloroform Over a 2% Platinum Alumina Catalyst," *Ind. Eng. Chem. Res.*, **32**, 1024 (1993).

Satterfield, C. N., *Mass Transfer in Heterogeneous Catalysis*, MIT Press, London (1970).

Schneider, R., D. Kiessling, G. Wendt, W. Burckhardt, and G. Winterstein, "Perovskite-Type Oxide Monolith Catalysts for Combustion of Chlorinated Hydrocarbons," *Catal. Today*, **47**, 429 (1999).

Sidebottom, H., and J. Franklin, "The Atmospheric Fate and Impact of Hydrofluorocarbons and Chlorinated Solvents," *Pure Appl. Chem.*, **68**, 1757 (1996).

Singuin, G., C. Petit, S. Libs, J. P. Hindermann, and A. Kiennemann, "Catalytic Destruction of Chlorinated Volatile Organic Compounds (CVOCs) Reactivity, Oxidation and Hydrolysis Mechanisms," *Appl. Catal. B*, **27**, 105 (2000).

Spivey, J. J., "Complete Catalytic Oxidation of Volatile Organics," *Ind. Eng. Chem. Res.*, **26**, 2165 (1987).

Storaro, L., R. Ganzerla, M. Lenarda, R. Zanoni, A. J. López, P. Olivera-Pastor, and E. R. Castellón, "Catalytic Behaviour of Chromia and Chromium Doped Alumina Pillared Clay Materials for the Vapor Phase Deep Oxidation of Chlorinated Hydrocarbons," *J. Mol. Catal. A*, **115**, 329 (1997).

Tajima, M., M. Niwa, Y. Fujii, Y. Koinuma, R. Aizawa, S. Kushiyama, S. Kobayashi, K. Mizuno, and H. Ohûchi, "Decomposition of Chlorofluorocarbons in the Presence of Water over Zeolite Catalyst," *Appl. Catal. B*, **9**, 167 (1996).

Taylor, P. H., and B. Dellinger, "Thermal Degradation Characteristics of Chloromethane Mixtures," *Environ. Sci. Technol.*, **22**, 438 (1988).

US EPA, *Needs for Eleven TRI Organic Chemical Groups*, Environmental Protection Agency, Pollution Prevention Research, Washington, DC (1991).

Van den Brink, R. W., P. Mulder, R. Louw, G. Sinquin, C. Petit, and J. P. Hindermann, "Catalytic Oxidation of Dichloromethane on γ-Al_2O_3: A Combined Flow and Infrared Spectroscopic Study," *J. Catal.*, **180**, 153 (1998).

Windawi, H., and M. Wyatt, "Catalytic Destruction of Halogenated Volatile Organic Compounds: Mechanisms of Platinum Catalyst Systems," *Platinum Met. Rev.*, **37**, 186 (1993).

Manuscript received Feb. 7, 2002, and revision received July 11, 2002.